applied sciences

MDPI

Article

The C-3 Functionalization of 1*H*-Indazole through Suzuki–Miyaura Cross-Coupling Catalyzed by a Ferrocene-Based Divalent Palladium Complex Immobilized over Ionic Liquid, as Well as Theoretical Insights into the Reaction Mechanism

Jinmeng Yu [1,2,3], Aqun Zheng [2], Lu Jin [1,*], Yong Wu [2,3], Qin Pan [2,3], Xiangdong Wang [2,3], Xiaoyong Li [2,3], Wanqin Wang [2,3], Min Gao [2,3] and Yang Sun [2,3,*]

[1] College of Chemistry and Chemical Engineering, Xinjiang Agricultural University, No. 311, Nongda East Road, Urumqi 830052, China
[2] Department of Applied Chemistry, School of Chemistry, Xi'an Jiaotong University, No. 28, Xianning West Road, Xi'an 710049, China
[3] Xixian New District Xingyi Advanced Materials Technology Co., Ltd., Room 1046, 1st Floor, Hongdelou, Building No. 20, Science and Technology Innovation Port, Western China, Fengxi New City, Xixian New District, Xi'an 712000, China
* Correspondence: lu_lu_jin@163.com (L.J.); sunyang79@mail.xjtu.edu.cn (Y.S.); Tel.: +86-29-82663914 (Y.S.); Fax: +86-29-82668559 (Y.S.)

Abstract: The C-3 functionalization of 1*H*-indazole could produce a lot of highly valuable pharmaceutical precursors, which could be used for the treatment of cancer and many other inflammatory diseases. This work was focused on the C-3 functionalization of 1*H*-indazole through Suzuki–Miyaura cross-coupling of 3-iodo-1*H*-indazole with organoboronic acids, catalyzed by various palladium catalysts immobilized over imidazolium ionic liquids, as well as catalyst recycling. A series of reaction parameters, including the substrate, catalyst, and ionic liquid, were fully investigated. It is significant to note that the yields of the present Suzuki–Miyaura cross-coupling were mainly determined by the catalyst and the solvent used, more than the chemical structure of the substrate. Furthermore, ferrocene-based divalent palladium complexes showed better catalytic outputs compared to simple palladium salts. Moreover, using two imidazolium ionic liquids, BMImX (BMIm$^+$ = 1-*n*-butyl-3-methylimidazolium, X$^-$ = BF_4^-, PF_6^-) not only improved the yields of cross-coupled products, but also avoided the formation of $Pd^{(0)}$ black, as compared to the non-ionic liquid facilitated reactions, and simultaneously making catalyst recycling more effective. On average, $BMImBF_4$ performed better than $BMImPF_6$. Additionally, scientific calculations revealed that 1,1′-bis(diphenylphosphino)ferrocene-palladium(II)dichloride dichloromethane complex ($PdCl_2$(dppf)) showed a lower energy barrier in the formation of intermediates than [1,1′-bis(di-*tert*-butylphosphino)ferrocene]dichloropalladium(II) ($PdCl_2$(dtbpf)), leading to higher catalytic outputs. This work may contribute to the development of 1*H*-indazole-derived new pharmaceuticals.

Keywords: Suzuki-Miyaura coupling; divalent palladium complex; 1*H*-indazole; ionic liquid; catalyst recycling

check for updates

Citation: Yu, J.; Zheng, A.; Jin, L.; Wu, Y.; Pan, Q.; Wang, X.; Li, X.; Wang, W.; Gao, M.; Sun, Y. The C-3 Functionalization of 1*H*-Indazole through Suzuki–Miyaura Cross-Coupling Catalyzed by a Ferrocene-Based Divalent Palladium Complex Immobilized over Ionic Liquid, as Well as Theoretical Insights into the Reaction Mechanism. *Appl. Sci.* **2023**, *13*, 4095. https://doi.org/10.3390/app13074095

Academic Editor: Raed Abu-Reziq

Received: 4 March 2023
Revised: 20 March 2023
Accepted: 22 March 2023
Published: 23 March 2023

1. Introduction

Indazoles, as a series of nitrogen-containing bicyclic compounds, are composed of an electron-rich pyrazole, along with a fused benzene ring [1]. Indazole has a ten-π electron aromatic heterocyclic structure, including two tautomers, 1*H*-indazole and 2*H*-indazole (Figure 1a,b) [1,2]. It was previously reported that 1*H*-indazole seems much more thermodynamically stable and abundant than 2*H*-tautomer in both the gas phase and aqueous solution; however, some 2*H*-indazole derivatives are also found in nature,

although their appearance is rare [2]. In practice, both 1*H*- and 2*H*-indazole derivatives have shown great potential for pharmaceutical applications (Figure 1c–e).

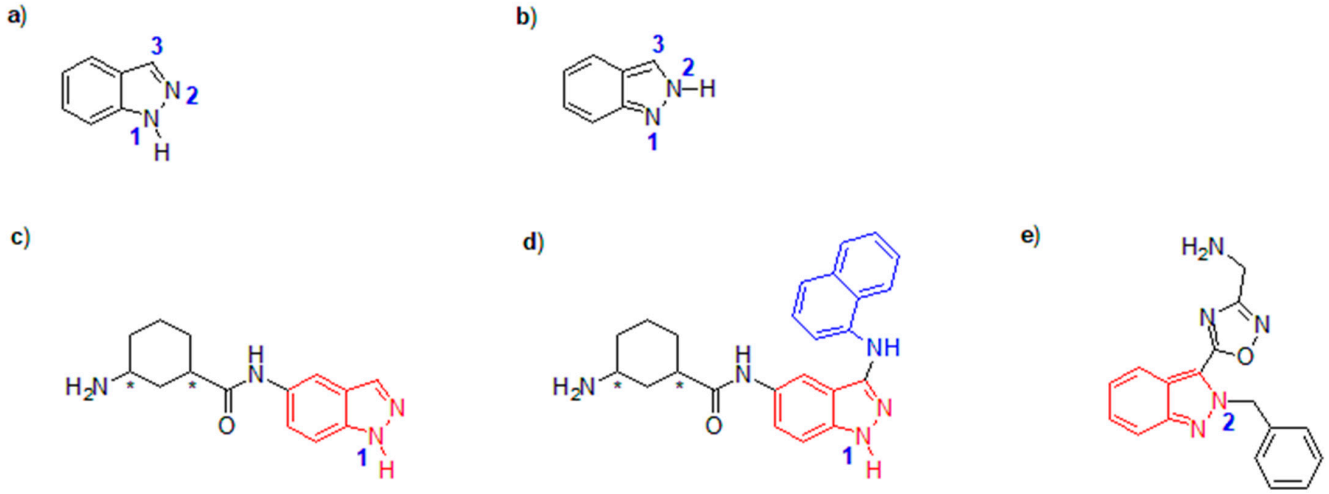

Figure 1. The tautomers of indazole, as well as 1*H*- and 2*H*-indazoles-derived potential pharmaceuticals: (**a**) 1*H*-indazole; (**b**) 2*H*-indazole; (**c**) **SR-17398** (anticancer), ULK1 inhibitor IC_{50} = 22.4 μmol L^{-1}, * mixture of 4 stereoisomers; (**d**) **SR-17398 derivative** (anticancer), ULK1 inhibitor IC_{50} = 45 nmol L^{-1}, * mixture of 4 stereoisomers; (**e**) Neuroprotective sodium channel modulator.

Overall, the pharmaceutical value of 1*H*-indazoles mainly lies in their antitumor activities [3], while 2*H*-indazole and its derivatives exhibit more versatile bioactivities, such as anticancer, antiplatelet, antiproliferative, anti-tubercular, antimalarial, antimicrobial, antiviral, and anti-inflammatory activities [4]. For example, cancer has been proven to be a disease marked by uncontrollable growth of abnormal cells in the human body, which can be initiated in any organ of the body and further transferred to distant organs [3]. In recent years, it has been proposed that one of the most probable pathways leading to this disease is the mutation of various types of genes and kinases (such as BRAF or KIT, etc.), causing diverse cellular anomalies and leading to the occurrence of cancer [3]. In practice, in addition to the traditional treatments for cancer using surgery, radiation therapy, chemotherapy, immunotherapy, or hormonal therapy, inhibition of kinase activity through blocking its improper phosphorylation represents a highly promising method for curing cancer [5]. 1*H*-indazole compounds have been selected as potential kinase inhibitors for treatment of cancer, mainly because their nitrogen-containing and other steric and electronic properties can deform the configuration of target protein kinase through formations of hydrogen bond, π-π stacking, or coordination linkage [6].

On the other hand, although the natural abundance of 2*H*-indazole is lower than that of 1*H*-indazole, the pharmaceutical potentials of 2*H*-indazole are still very attractive, probably owing to its unique nitrogen-containing heterocyclic structure, which can bind to protein kinase, affecting the progress of many diseases [2]. Therefore, on the basis of these findings, synthesizing both functional 1*H*- and 2*H*-indazole derivatives could contribute to the development of new pharmaceuticals.

The present developments in the synthetic functionalization of both 1*H*- and 2*H*-indazole can be generally divided into three patterns, including N- and C-functionalization, as well as fused cyclization [7]. N-functionalization means the catalytic coupling of the N-H group of indazole with electrophiles, leading to production of alkylation and arylation [8]. The C-functionalization of indazole refers to the alkylation [9], arylation [10], alkoxylation [11], amination [12], halogenation [13], and phosphonylation [14] of C-3 of indazole in a catalytic or photocatalytic manner.

Lastly, some specially functionalized indazole derivatives, such as 3-aminoindazole, can be reacted with enaminone and bromodifluoroacetic acid through three-component cy-

clization, leading to a fused-ring compound [15]. In light of radical capture experiments, the mechanism was illustrated as addition-elimination mechanism (S_NV) mode [15]. Generally speaking, chemical functionalization of indazole usually demands a catalyst, along with an appropriate solvent, temperature, and reaction time, meaning that future large-scale production would involve many economic and environmental issues.

The C-functionalization carried out on C-3 position of 1*H*-indazole played a key role in promoting the pharmaceutical activity of indazole derivatives. For example, the abnormal ignition (phosphorylation) of unc-51-like kinase 1 (ULK1), a ubiquitously expressed protein activated by stress-induced autophagy under many conditions, decreases the efficiency of the current chemotherapeutics for cancer, and meanwhile increases the growth of cancer [16]. Therefore, using small molecule inhibitors of ULK1 such as SR-17398 (Figure 1c) could block the phosphorylation of ULK1 and simultaneously enhance the effect of chemotherapy [17]. The backbone of SR-17398 is indazole, whose nitrogen-containing heterocyclic structure can deform the configuration of ULK1, finally blocking the activation of ULK1 [18]. However, if the C-3 position of indazole on SR-17398 is functionalized by introducing a 1-naphthylamino group (Figure 1d), the half inhibitory concentration (IC_{50}) is greatly decreased, and the C-3 position of indazole showed an influence on the inhibitory deformation of ULK1 [18]. On the other hand, C-3 functionalized 2*H*-indazole also showed high activity for the treatment of neurological diseases (Figure 1e) [19]. Functionalization of C-3 of indazoles allows developing new and powerful pharmaceuticals.

In practice, direct functionalization of C-3 on 1*H*-indazole suffers from several drawbacks. First, direct C-3 alkylation of 1*H*-indazole through the Minisci reaction (addition of nucleophilic carbon radical to protonated electron-deficient aromatic heterocycle) produced a very low yield, which can be ascribed to the unique electronic structure of the five-membered nitrogen-containing heterocycle [20]. Next, direct C-3 arylation of 1*H*-indazole required an uncommon catalyst and challenging reaction conditions [4]. These results delay progress to large-scale production. All in all, in view of the present progress in C-3 functionalization, exploring new synthetic methods deserves more attention.

The Suzuki–Miyaura cross-coupling reaction represents a palladium (Pd)-catalyzed C-C bond formation, already standing as a powerful methodology for the construction of sophisticated molecules for the last two decades [21,22]. First of all, taking into account the mechanism of Pd-catalyzed Suzuki–Miyaura coupling of aryl halide with organoboronic acid, a $Pd^{(0)}$ to $Pd^{(II)}$ cycle is widely accepted as the most reasonable pathway [22]. In detail, the oxidative addition of aryl halide to $Pd^{(0)}$ generates a $Pd^{(II)}$ intermediate, while the transmetalation of the $Pd^{(II)}$ intermediate, followed by the reductive elimination, produces the coupled product and regenerates the active $Pd^{(0)}$ [22,23].

Next, Pd-catalyzed Suzuki–Miyaura coupling has shown several significant advantages, particularly regarding its broad functional group tolerance and mild reaction conditions [24,25]. For instance, the suitable electrophiles cover sterically congested molecules, inert aryl, and vinyl chlorides, as well as sulfonate derivatives, while the nucleophiles also include thermally unstable polyfluorophenyl and 2-heteroaryl boron reagents [25]. Meanwhile, the organoboron compounds (electrophile) exhibit high stabilities towards air and moisture [24]. Therefore, although 1*H*-indazole has a sophisticated nitrogen-containing heterocycle, it is promising to develop Pd-catalyzed Suzuki–Miyaura coupling reaction for C-3 functionalization of 1*H*-indazole.

On the other hand, the recovery and recycling of Pd catalysts has not been well addressed. Herein, depending on the catalyst precursor, the known Pd catalytic systems can be divided into homogeneous and heterogeneous systems. The former series mainly refers to soluble Pd salts or complexes having various ligands, including phosphine and N-heterocyclic carbenes [25], while the latter usually signifies the Pd nanoparticles, clusters, or single atoms immobilized over solid supports such as silica, polymers, or activated carbon [26]. No matter which kind of catalyst is used, the active Pd species usually shows a tendency to be reduced and subsequently agglomerated to inactive $Pd^{(0)}$ black during catalysis [26,27]. In order to decrease this unfavorable inclination, ionic nitrogen compounds

such as ammonium, amidinium, and pyridinium salts were ever introduced to stabilize the active Pd ($Pd^{(0)}$ or Pd^{2+}) species, where the effects of stabilization, fixation, modulation of catalyst morphology, and reaction medium, as well as phase-transfer property on catalysis, were highly anticipated [26]. However, this endeavor was not completely effective, and quite a few ionic nitrogen compounds showed inhibitory rather than accelerating or stabilizing effects on the Pd-catalyzed reactions [26]. Obviously, there is still a lot of room to explore efficient methods to immobilize expensive Pd catalysts for recycling.

Traditionally, immobilization of Pd salts or complexes into solid supports has created heterogeneous catalysts for the Suzuki–Miyaura coupling reaction, and sometimes solid supports can serve as base generated in situ in the catalytic reaction [26]. However, the immobilization present cannot avoid leaching and the degradation of the Pd catalyst, probably because the dispersion of solvent (water and organic molecules) into the pores of solid support, which destroys the chemical or physical linkage between the Pd component and support [26]. Therefore, in order to securely fix Pd, new support materials, instead of the common solid supports (silicate, aluminum oxide or other known solid acids), deserve further exploration.

The catalysis carried out in ionic liquids (ILs) has experienced a tremendous growth over the past two decades [28]. There are numerous examples of versatile catalytic reactions that have been effectively accomplished in this kind of media [28]. Theoretically, room temperature ionic liquids (usually denoted as RTILs or ILs) are composed of ions with melting points lower than 100 °C, which are nonvolatile, nonflammable, chemically stable, easy to recover, and eco-friendly for many chemical reactions, arousing much interest in their usage as either a catalyst or solvent [28,29].

Furthermore, the great enthusiasm for exploring ILs in catalysis has not only been propelled by the eco-friendly properties of ILs, but also owing to the unique polar or ionic nature of ILs, which the common molecular solvents do not show, subsequently immobilizing catalytic components tightly and lastingly [28,30]. Therefore, the leaching of catalytically active components from ILs would become slower and minimal, product extraction and purification become more convenient, and the catalyst activity could be retained for a long time [31]. Meanwhile, certain catalytic reactions that cannot be performed in common organic solvents seem more possible in ILs [32].

Due to the demand for developing new 1*H*-indazole-derived pharmaceuticals, the present low efficiency of C-3 functionalization of 1*H*-indazole, as well as the high potential of Pd-catalyzed Suzuki–Miyaura coupling in ILs, this work aimed to develop the C-3 functionalization of 1*H*-indazole reactions using Pd-catalyzed Suzuki–Miyaura coupling. In order to improve the recovery and recycling of the Pd catalyst, a series of imidazolium ILs BMImX ($BMIm^+$ = 1-*n*-butyl-3-methylimidazolium; X^- = PF_6^-, BF_4^-) were introduced as a support material, which not only had controllable hydrophilicity, owing to variation of the anions, but also contained a nitrogen atom, showing coordination effects for stabilizing Pd ions. Lastly, on the basis of theoretical calculations, the catalytic mechanism was summarized, and comparison of Pd catalysts was carried out. In general, this work demonstrates a new and recyclable strategy for C-3 functionalization of 1*H*-indazole, contributing to the development of indazole-based pharmaceuticals.

2. Experimental

2.1. Starting Materials

1*H*-indazole (98%), di-*tert*-butyl dicarbonate ($(Boc)_2O$, 99%), 4-dimethylaminopyridine (DMAP, 99%), 2-furanboronic acid (97%; compound **4**, Scheme 1), 4-methoxycarbonylphenylboronic acid (97%; compound **7**, Scheme 1), 3-methoxycarbonylphenylboronic acid (97%; compound **10**, Scheme 1), lithium hydroxide monohydrate ($LiOH{\cdot}H_2O$, 98%) were bought from Shanghai Macklin Biochemical Technology Co., Ltd. (Shanghai, China) and used without purification.

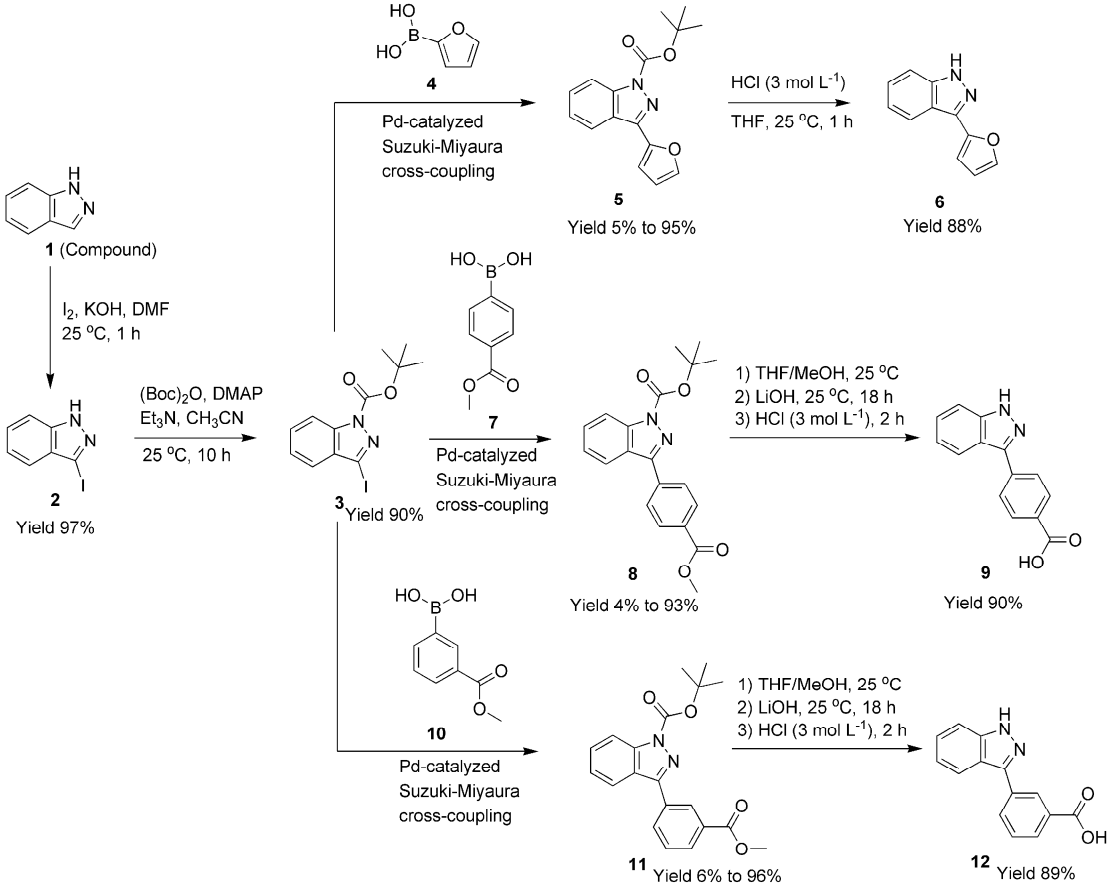

Scheme 1. C-3 functionalization of 1*H*-indazole through a catalytic Suzuki–Miyaura cross-coupling reaction.

Tetrakis(triphenylphosphine)palladium(0) ($Pd(PPh_3)_4$, 99%), palladium(II) acetate ($Pd(OAc)_2$, 99% purity, Pd 47%), palladium(II) chloride ($PdCl_2$, 99% purity, Pd 59%), 1,1′-bis(diphenylphosphino) ferrocene-palladium(II)dichloride dichloromethane complex ($PdCl_2$(dppf), 98% purity, Pd >13%), and [1,1′-bis(di-*tert*-butylphosphino)ferrocene]dichloropalladium(II) ($PdCl_2$(dtbpf), 98%) were all commercially available from Sigma-Aldrich (St. Louis, MO, USA). Two imidazolium ILs, BMImX ($BMIm^+$ = 1-*n*-butyl-3-methylimidazolium; X^- = BF_4^-, PF_6^-; both 98% purities) were bought from Alfa. Deuterium reagents used in NMR, including $CDCl_3$, CD_3OD, and DMSO-d_6, were purchased from Shanghai Macklin Biochemical Technology Co., Ltd. and used without purification. Other organic solvents were provided by local distributors and used after purification in our laboratory.

2.2. Analytical Instruments

The melting points of compounds **2**, **3**, **5**, **6**, **8**, **9**, **11**, and **12** (Scheme 1) were tested using WRR-Y melting point apparatus, Shanghai INESA Physico-Optical Instrument Co., Ltd. (Shanghai, China). ^{1}H NMR was tested on a Bruker ADVANCE III instrument (400 MHz), ^{13}C NMR was measured on a Bruker ADVANCE III instrument (101 MHz). ESI-HRMS was obtained on micrOTOF-Q II, Bruker Daltonics equipment (Bremen, Germany). The ESI-HRMS of compounds **9** and **12** was tested using time of flight secondary ion mass spectrometry (TOF-SIMS), M6, IONTOF equipment (Münster, Germany). The C, H, and N elemental analyses were performed on an Elementar VarioEL III instrument, Elementar equipment (Langenselbold, Germany). The FT-IR spectra of the synthesized samples were taken in potassium bromide pellets using a Bruker Tensor 27 spectrometer, BRUKER equipment (Bremen, Germany).

2.3. Synthesis of 3-Iodo-1H-indazole (Compound **2**)

As shown in Scheme 1, 3-iodo-1*H*-indazole (compound **2**) was prepared by iodination of 1*H*-indazole (compound **1**), according to a previous method developed by Bocchi and Palli [33]. In practice, iodine (16.0 g, 0.064 mol) and potassium hydroxide pellets (6.72 g, 0.12 mol) were combined with a DMF solution (60 mL) of indazole (3.77 g, 0.032 mol) at 25 °C under magnetic stirring for 1 h. The reaction mixture was then poured into aqueous $NaHSO_3$ (10%, 200 mL) and extracted with diethyl ether (2 × 150 mL). The combined organic layers were washed with distilled water (2 × 150 mL) and brine (2 × 150 mL) and dried over anhydrous $MgSO_4$, and the organic solvent was evaporated under reduced pressure, to give a light yellow solid (7.28 g, yield of 97%). Mp 142.7–144.3 °C (lit. mp 141 °C [34]). ^{1}H NMR (400 MHz, Methanol-d_4) δ_H, ppm: 7.50 (1H, dt, *J* = 1.7, 7.4 Hz, Ar*H*), 7.44 (1H, d, *J* = 1.7 Hz, Ar*H*), 7.43 (1H, d, *J* = 1.7 Hz, Ar*H*), 7.19 (1H, m, Ar*H*) (Figure S1, Section S1, Supplementary Materials). ^{13}C NMR (101 MHz, CD_3OD) δ_C, ppm: 140.75, 127.55, 127.19, 121.32, 120.60, 110.07, 92.02 (Figure S2, Section S2, Supplementary Materials). Anal. Calcd for $C_7H_5N_2I$: C, 34.42; H, 2.04; N, 11.47. Found: C, 34.54; H, 1.64; N, 11.37. FT-IR (KBr) σ, cm^{-1}: 3153 (vs, N-H), 1620 (s, C=N), 1319 (s, C-N), 424 (m, C-I).

2.4. Synthesis of Tert-butyl-3-iodo-1H-indazole-1-carboxylate (Compound **3**)

As shown in Scheme 1, 3-iodo-1*H*-indazole (compound **2**, 1.22 g, 5 mmol), $(Boc)_2O$ (1.2 g, 5.5 mmol), DMAP (30 mg, 0.24 mmol), and triethylamine (1.1 mL, 0.76 g, 7.5 mmol) were combined with CH_3CN (10 mL) in a round-bottom flask (250 mL) with a condenser and sealed with a balloon. After vigorous stirring for 10 h at 25 °C, the dark orange solution was evaporated to dryness under reduced pressure, to completely remove the solvent and triethylamine. The residue was re-dissolved in diethyl ether (150 mL), then washed with brine (2 × 50 mL), dried over anhydrous $MgSO_4$, and then concentrated under reduced pressure. Crude product was purified using flash chromatography (SiO_2, 100–200 mesh; petroleum ether/ethyl acetate, 5/1, *v*/*v*; adding a few drops of triethylamine in eluent, 10 drops of triethylamine vs. 200 mL eluent) to give pure compound **3** (yellow oil, solidified overnight; 1.54 g, 90% yield). Mp 117.2–119.5 °C. ^{1}H NMR (400 MHz, $CDCl_3$) δ_H, ppm: 1.72 (9H, s, *tert*-butyl), 7.38 (1H, t, *J* = 8.0 Hz, Ar*H*), 7.50 (1H, d, *J* = 8.0 Hz, Ar*H*), 7.59 (1H, t, *J* = 7.6 Hz, Ar*H*), 8.11 (1H, d, *J* = 8.4 Hz, Ar*H*) (Figure S3, Section S3, Supplementary Materials). ^{13}C NMR (101 MHz, $CDCl_3$) δ_C, ppm: 148.44, 139.67, 130.26, 130.07, 124.29, 122.07, 114.64, 103.05, 85.59, 28.22 (Figure S4, Section S4, Supplementary Materials). ESI-HRMS (positive, *m*/*z*): 366.9901 (Calcd. for $[M+Na]^+$ 367.1374) and 711.0117 (Calcd. for $[2M+Na]^+$ 711.2851) (Figure S5, Section S5, Supplementary Materials). Anal. Calcd for $C_{12}H_{13}N_2O_2I$: C, 41.86; H, 3.77; N, 8.13. Found: C, 41.85; H, 3.22; N, 8.25. FT-IR (KBr) σ, cm^{-1}: 2983 (s, methyl on *tert*-butyl), 1726 (vs, C=O), 1610 (m, C=N), 1381 (vs, C-N), 1234 (vs, C-O) (Figure S6, Section S6, Supplementary Materials).

2.5. Synthesis of Tert-butyl-3-(2-furyl)-1H-indazole-1-carboxylate (Compound **5**)

As shown in Scheme 1, compound **5** was obtained through a Pd-catalyzed Suzuki–Miyaura coupling reaction, which is comprehensively described in Section 2.11. Yellow oils (yields of 5–95%, Table 1 and Figure 2). ^{1}H NMR (400 MHz, $CDCl_3$) δ_H, ppm: 1.77 (9H, s, *tert*-butyl), 7.41 (1H, d, *J* = 8.0 Hz, Ar*H*), 7.49–7.51 (3H, m, Ar*H*), 7.54–7.59 (2H, m, *H* on furyl), 8.21 (1H, t, *J* = 9.2 Hz, *H* on furyl) (Figure S7, Section S7, Supplementary Materials). ^{13}C NMR (101 MHz, $CDCl_3$) δ_C, ppm: 149.35, 147.77, 143.61, 141.63, 140.61, 129.19, 124.14, 123.41, 122.12, 114.81, 111.81, 110.16, 85.16, 28.25 (Figure S8, Section S8, Supplementary Materials). ESI-HRMS (positive, *m*/*z*): 307.1028 (Calcd. for $[M+Na]^+$ 307.2989) (Figure S9, Section S9, Supplementary Materials). Anal. Calcd for $C_{16}H_{16}N_2O_3$: C, 67.60; H, 5.63; N, 9.86. Found: C, 68.21; H, 6.22; N, 9.25. FT-IR (KBr) σ, cm^{-1}: 3156 (m, furyl), 2972 (m, methyl on *tert*-butyl), 1738 (vs, C=O), 1614 (m, C=N), 1510 (m, furyl), 1422 (m, furyl), 1374 (vs, C-N), 1243 (vs, C-O) (Figure S10, Section S10, Supplementary Materials).

Table 1. Catalytic Suzuki–Miyaura cross-coupling of compounds **3** with **4**.

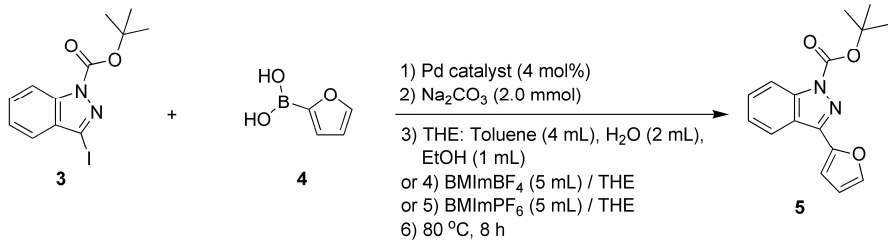

Entry [a]	Catalyst [b]	Solvent	Conversion (%) [c]	Yield (%) [d]
1	$Pd(PPh_3)_4$	THE [a]	5	5
2		$BMImBF_4$/THE	21	21
3		$BMImPF_6$/THE	23	23
4	$Pd(OAc)_2$	THE	34	34
5		$BMImBF_4$/THE	51	51
6		$BMImPF_6$/THE	42	42
7	$PdCl_2$	THE	19	19
8		$BMImBF_4$/THE	55	55
9		$BMImPF_6$/THE	40	40
10	$PdCl_2$(dppf)	THE	85	85
11		$BMImBF_4$/THE	95	95
12		$BMImPF_6$/THE	79	79
13	$PdCl_2$(dtbpf)	THE	90	90
14		$BMImBF_4$/THE	88	88
15		$BMImPF_6$/THE	82	82

[a] Reaction conditions (details as in Section 2.11.): electrophile **3** (1.0 mmol), nucleophile **4** (1.2 mmol), Pd catalyst (4 mol%, based on organic halide), THE solvent system (Toluene, 4 mL; H_2O, 2 mL; EtOH, 1 mL), Na_2CO_3 (2.0 mmol), ILs ($BMImPF_6$ or $BMImBF_4$, 5 mL); 80 °C, 8 h. [b] $Pd(PPh_3)_4$, tetrakis(triphenylphosphine)palladium(0); $Pd(OAc)_2$, palladium(II) acetate; $PdCl_2$, palladium(II) chloride; $PdCl_2$(dppf), 1,1′-bis(diphenylphosphino)ferrocene-palladium(II)dichloride dichloromethane; $PdCl_2$(dtbpf), [1,1′-bis(di-*tert*-butylphosphino)ferrocene]dichloropalladium(II). [c] Conversion of electrophile **3** (%). [d] Isolated yield (%) of compound **5** (*tert*-butyl-3-(2-furyl)-1*H*-indazole-1-carboxylate), based on compound **3**. No by-products were found with flash chromatography for all entries in this table.

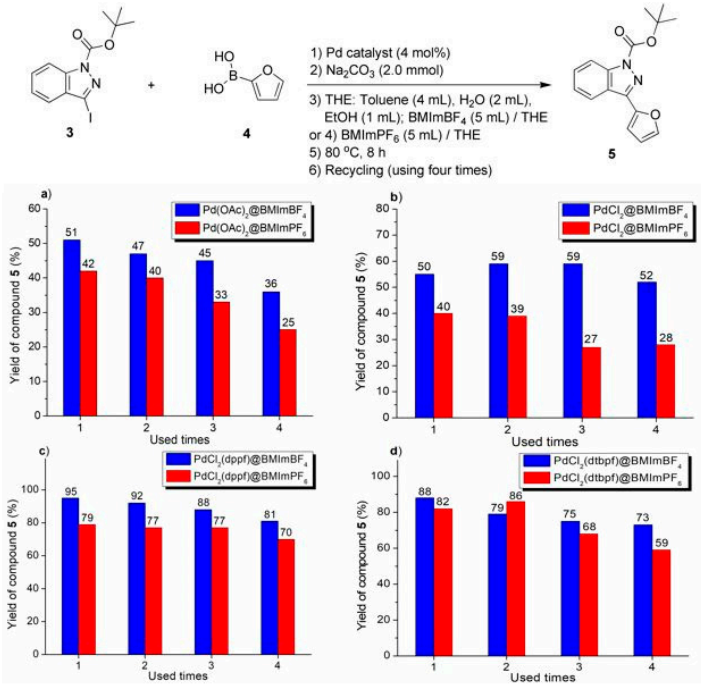

Figure 2. Recycling experiments on Suzuki–Miyaura cross-coupling of compounds **3** with **4** catalyzed by Pd catalyst, immobilized over imidazolium ionic liquid: (**a**) $Pd(OAc)_2$ over ILs; (**b**) $PdCl_2$ over ILs; (**c**) $PdCl_2$(dppf) over ILs; (**d**) $PdCl_2$(dtbpf) over ILs.

2.6. Synthesis of 3-(2-Furyl)-1H-indazole (Compound **6***)*

As shown in Scheme 1, compound **5** (0.586 g, 2 mmol) was dissolved in THF (5 mL) under continuous stirring at 25 °C, the solution was then acidified through dropwise addition of HCl solution (3 mol/L) until the pH value reached 2. After stirring for 1 h, the mixture was diluted with CH_2Cl_2 (100 mL), the organic layer was separated and washed with brine (100 mL), dried over anhydrous Na_2SO_4, and concentrated under reduced pressure. The residue was purified using flash chromatography (SiO_2, 100–200 mesh; petroleum ether/ethyl acetate 5/1, *v*/*v*, adding a few drops of triethylamine in eluent, 10 drops of triethylamine vs. 200 mL eluent) to give compound **6** (yellow solid, 0.33 g, yield of 88%). Mp 163.6–164.2 °C (lit. mp 165–166 °C [35]). ^{1}H NMR (400 MHz, $CDCl_3$) δ_H, ppm: 8.00 (1H, d, *J* = 8.2 Hz, Ar*H*), 7.58 (1H, d, *J* = 1.8 Hz, Ar*H*), 7.43 (1H, d, *J* = 8.4 Hz, *H* on furyl), 7.31 (1H, t, *J* = 7.6 Hz, Ar*H*), 7.11 (1H, t, *J* = 7.6 Hz, Ar*H*), 6.87 (1H, d, *J* = 3.4 Hz, *H* on furyl), 6.50 (1H, dd, *J* = 1.8, 3.4 Hz, *H* on furyl) (Figure S11, Section S11, Supplementary Materials). ^{13}C NMR (101 MHz, $CDCl_3$) δ_C, ppm: 148.96, 142.29, 141.29, 136.92, 126.93, 121.21, 120.93, 119.64, 111.15, 109.93, 106.64 (Figure S12, Section S12, Supplementary Materials). ESI-HRMS (positive, *m*/*z*): 207.0504 (Calcd. for $[M+Na]^+$ 207.1834). Anal. Calcd for $C_{11}H_8N_2O$: C, 71.74; H, 4.34; N, 15.21. Found: C, 72.01; H, 4.29; N, 15.28. FT-IR (KBr) σ, cm^{-1}: 3626 (br m, N-H), 3154 (m, furyl ring), 1617 (m, C=N), 1387 (m, C-N), 1234 (m, C-O).

2.7. Synthesis of Tert-butyl-3-(4-(methoxycarbonyl)phenyl)-1H-indazole-1-carboxylate (Compound **8***)*

As shown in Scheme 1, compound **8** was obtained through a Pd-catalyzed Suzuki–Miyaura coupling reaction, which is described comprehensively in Section 2.11. Mp 73.8–75.1 °C (white solids, yields of 4–93%, Table 2 and Figure 3). ^{1}H NMR (400 MHz, $CDCl_3$) δ_H, ppm: 1.75 (9H, s, *tert*-butyl), 3.96 (3H, s, CH_3), 7.38–7.42 (1H, m, Ar*H*), 7.58 (1H, t, *J* = 8.0 Hz, Ar*H*), 7.99 (1H, d, *J* = 8.0 Hz, Ar*H*), 8.09 (2H, d, *J* = 8.0 Hz, Ar*H*), 8.20 (3H, t, *J* = 8.4 Hz, Ar*H*) (Figure S13, Section S13, Supplementary Materials). ^{13}C NMR (101 MHz, $CDCl_3$) δ_C, ppm: 166.84, 149.33, 148.69, 141.16, 136.51, 130.68, 130.14, 129.05, 128.25, 124.25, 124.10, 121.27, 115.11, 85.27, 52.36, 28.26 (Figure S14, Section S14, Supplementary Materials). ESI-HRMS (positive, *m*/*z*): 353.1492 (Calcd. for $[M+H]^+$ 353.3909) and 727.2764 (Calcd. for $[2M+Na]^+$ 727.7557) (Figure S15, Section S15, Supplementary Materials). Anal. Calcd for $C_{20}H_{20}N_2O_4$: C, 68.18; H, 5.68; N, 7.95. Found: C, 69.01; H, 5.21; N, 7.20. FT-IR (KBr) σ, cm^{-1}: 2929 (m, methyl on *tert*-butyl), 1695 (vs, C=O), 1647 (m, C=N), 1390 (m, C-N), 1230 (w, C-O) (Figure S16, Section S16, Supplementary Materials).

2.8. Synthesis of 4-(1H-Indazole-3-yl)benzoic Acid (Compound **9***)*

As shown in Scheme 1, compound **9** was obtained by saponification and subsequent deprotection of compound **8**, according to a previous report, with some modifications [36]. In practice, compound **8** (400 mg, 1.136 mmol) was dissolved into a mixed solution of THF (5 mL) with methanol (1 mL) under magnetic stirring at 25 °C. Then, the LiOH solution ($LiOH{\cdot}H_2O$ of 476 mg dissolved in distilled H_2O of 3 mL) was introduced. The resulting reaction mixture was further stirred at 25 °C for 18 h. When the time was up, the reaction mixture was acidified by dropping HCl solution (3 mol L^{-1}), until the pH value was adjusted to 2. The mixture thus obtained was stirred for 2 h, to remove the boc-group.

Table 2. Catalytic Suzuki–Miyaura cross-coupling of compounds **3** with **7**.

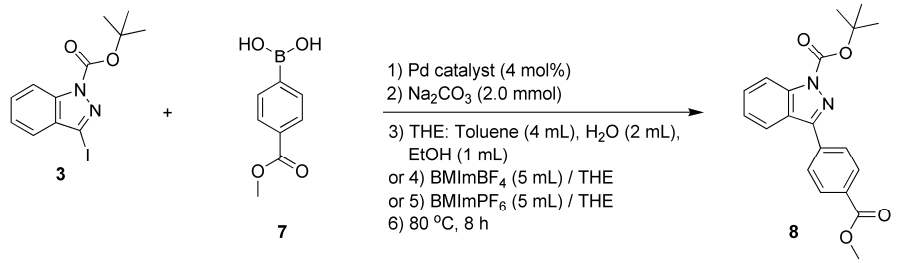

3 + **7** → **8**

Entry [a]	Catalyst [b]	Solvent	Conversion (%) [c]	Yield (%) [d]
1	$Pd(PPh_3)_4$	THE [a]	10	10
2		$BMImBF_4$/THE	4	4
3		$BMImPF_6$/THE	17	17
4	$Pd(OAc)_2$	THE	30	30
5		$BMImBF_4$/THE	59	59
6		$BMImPF_6$/THE	57	57
7	$PdCl_2$	THE	14	14
8		$BMImBF_4$/THE	62	62
9		$BMImPF_6$/THE	47	47
10	$PdCl_2$(dppf)	THE	86	86
11		$BMImBF_4$/THE	91	91
12		$BMImPF_6$/THE	89	89
13	$PdCl_2$(dtbpf)	THE	90	90
14		$BMImBF_4$/THE	93	93
15		$BMImPF_6$/THE	89	89

[a] Reaction conditions (details as in Section 2.11.): electrophile **3** (1.0 mmol), nucleophile **7** (1.2 mmol), Pd catalyst (4 mol%, based on organic halide), THE solvent system (Toluene, 4 mL; H_2O, 2 mL; EtOH, 1 mL), Na_2CO_3 (2.0 mmol), ILs ($BMImPF_6$ or $BMImBF_4$, 5 mL); 80 °C, 8 h. [b] $Pd(PPh_3)_4$, tetrakis(triphenylphosphine)palladium(0); $Pd(OAc)_2$, palladium(II) acetate; $PdCl_2$, palladium(II) chloride; $PdCl_2$(dppf), 1,1′-bis(diphenylphosphino)ferrocene-palladium(II)dichloride dichloromethane; $PdCl_2$(dtbpf), [1,1′-bis(di-*tert*-butylphosphino)ferrocene]dichloropalladium(II). [c] Conversion of electrophile **3** (%). [d] Isolated yield (%) of compound **8** (*tert*-butyl-3-(4-(methoxycarbonyl)phenyl)-1*H*-indazole-1-carboxylate), based on compound **3**. No by-products were found by flash chromatography for all entries in this table.

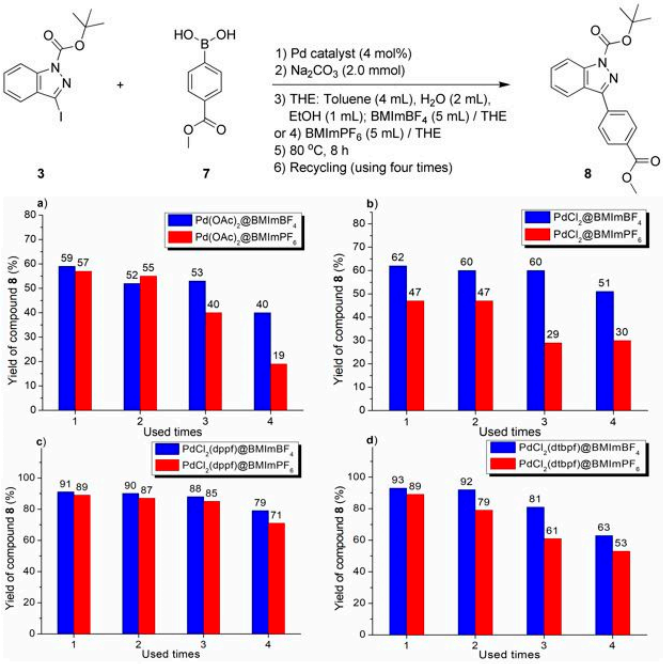

Figure 3. Recycling experiments on Suzuki–Miyaura cross-coupling of compounds **3** with **7** catalyzed by Pd catalyst immobilized over imidazolium ionic liquid: (**a**) $Pd(OAc)_2$ over ILs; (**b**) $PdCl_2$ over ILs; (**c**) $PdCl_2$(dppf) over ILs; (**d**) $PdCl_2$(dtbpf) over ILs.

Next, the reaction mixture was extracted with CH_2Cl_2 (3 × 50 mL), and the combined organic layers were dried over anhydrous $MgSO_4$ and then concentrated under reduced pressure. The residue was purified by flash chromatography (SiO_2, 100–200 mesh; dichloromethane/methanol = 10/1, *v*/*v*, adding a few drops of triethylamine, 10 drops of triethylamine vs. 200 mL eluent) to afford compound **9** (247 mg, yield of 90%) as a white solid. Mp >280 °C. ^{1}H NMR (400 MHz, DMSO-d_6) δ_H, ppm: 13.49 (1H, s, COO*H*), 8.11 (5H, dd, *J* = 8.3, 16.0 Hz, Ar*H*), 7.63 (1H, d, *J* = 8.4 Hz, Ar*H*), 7.43 (1H, m, Ar*H*), 7.24 (1H, m, Ar*H*) (Figure S17, Section S17, Supplementary Materials). ^{13}C NMR (101 MHz, DMSO-d_6) δ_C, ppm: 167.78, 142.65, 142.23, 138.48, 130.55, 130.18, 127.08, 126.84, 122.04, 121.14, 120.68, 111.37 (Figure S18, Section S18, Supplementary Materials). ESI-HRMS (TOF-SIMS, positive, m/z): 239.0815 (Calcd. for $[M+H]^+$ 239.2480) (Figure S19, Section S19, Supplementary Materials). Anal. Calcd. for $C_{14}H_{10}N_2O_2$: C, 70.58; H, 4.20; N, 11.76. Found: C, 71.33; H, 4.65; N, 12.25. FT-IR (KBr) σ, cm^{-1}: 3396 (br m, N-H), 2925 (m, furyl ring), 1696 (vs, C=O), 1611 (m, C=N), 1383 (m, C-N), 1254 (m, C-O).

2.9. Synthesis of Tert-butyl-3-(3-(methoxycarbonyl)phenyl)-1H-indazole-1-carboxylate (Compound **11***)*

As shown in Scheme 1, compound **11** was obtained through Pd-catalyzed Suzuki–Miyaura coupling of compounds **3** with **10**, which is comprehensively described in Section 2.11. Yellow oils (yields of 6–96%, Table 3 and Figure 4). ^{1}H NMR (400 MHz, $CDCl_3$) δ_H, ppm: 8.66 (1H, t, *J* = 1.8 Hz, Ar*H*), 8.20 (2H, m, Ar*H*), 8.13 (1H, d, *J* = 7.9 Hz, Ar*H*), 7.98 (1H, d, *J* = 8.2 Hz, Ar*H*), 7.57 (2H, m, Ar*H*), 7.38 (1H, t, *J* = 7.6 Hz, Ar*H*), 3.95 (3H, s, methyl), 1.74 (9H, s, *tert*-butyl) (Figure S20, Section S20, Supplementary Materials). ^{13}C NMR (101 MHz, $CDCl_3$) δ_C, ppm: 166.83, 149.40, 148.87, 141.12, 132.74, 132.50, 130.87, 130.39, 129.39, 129.09, 129.02, 124.19, 124.10, 121.33, 115.07, 85.18, 52.38, 28.28 (Figure S21, Section S21, Supplementary Materials). ESI-HRMS (positive, m/z): 353.1518 (Calcd. for $[M+H]^+$ 353.3909) (Figure S22, Section S22, Supplementary Materials). Anal. Calcd. for $C_{20}H_{20}N_2O_4$: C, 68.18; H, 5.68; N, 7.95. Found: C, 68.75.01; H, 5.38; N, 6.61. FT-IR (KBr) σ, cm^{-1}: 2983 (m, methyl on *tert*-butyl), 1729 (vs, C=O), 1649 (m, C=N), 1380 (m, C-N), 1246 (m, C-O) (Figure S23, Section S23, Supplementary Materials).

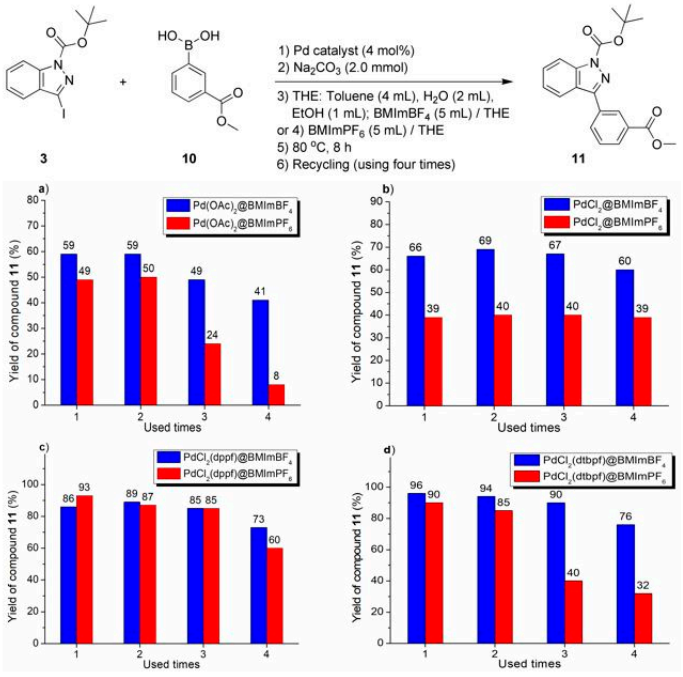

Figure 4. Recycling experiments on Suzuki–Miyaura cross-coupling of compounds **3** with **10**, catalyzed by Pd catalyst and immobilized over imidazolium ionic liquid: (**a**) $Pd(OAc)_2$ over ILs; (**b**) $PdCl_2$ over ILs; (**c**) $PdCl_2$(dppf) over ILs; (**d**) $PdCl_2$(dtbpf) over ILs.

Table 3. Catalytic Suzuki–Miyaura cross-coupling of compounds **3** with **10**.

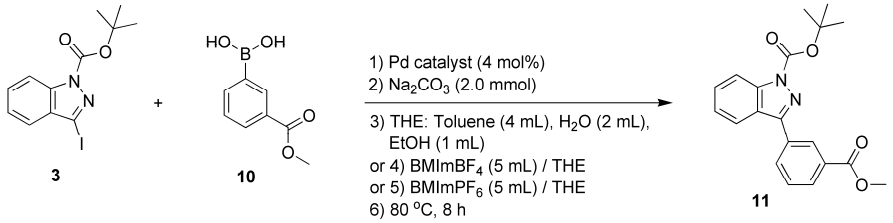

3 + **10** → **11**

Entry [a]	Catalyst [b]	Solvent	Conversion (%) [c]	Yield (%) [d]
1	$Pd(PPh_3)_4$	THE [a]	14	14
2		$BMImBF_4$/THE	6	6
3		$BMImPF_6$/THE	27	27
4	$Pd(OAc)_2$	THE	27	27
5		$BMImBF_4$/THE	59	59
6		$BMImPF_6$/THE	49	49
7	$PdCl_2$	THE	10	10
8		$BMImBF_4$/THE	66	66
9		$BMImPF_6$/THE	39	39
10	$PdCl_2$(dppf)	THE	82	82
11		$BMImBF_4$/THE	86	86
12		$BMImPF_6$/THE	93	93
13	$PdCl_2$(dtbpf)	THE	92	92
14		$BMImBF_4$/THE	96	96
15		$BMImPF_6$/THE	90	90

[a] Reaction conditions (details as in Section 2.11.): electrophile **3** (1.0 mmol), nucleophile **10** (1.2 mmol), Pd catalyst (4 mol%, based on organic halide), THE solvent system (Toluene, 4 mL; H_2O, 2 mL; EtOH, 1 mL), Na_2CO_3 (2.0 mmol), ILs ($BMImPF_6$ or $BMImBF_4$, 5 mL); 80 °C, 8 h. [b] $Pd(PPh_3)_4$, tetrakis(triphenylphosphine)palladium(0); $Pd(OAc)_2$, palladium(II) acetate; $PdCl_2$, palladium(II) chloride; $PdCl_2$(dppf), 1,1′-bis(diphenylphosphino)ferrocene-palladium(II)dichloride dichloromethane; $PdCl_2$(dtbpf), [1,1′-bis(di-*tert*-butylphosphino)ferrocene]dichloropalladium(II). [c] Conversion of electrophile **3** (%). [d] Isolated yield (%) of compound **11** (*tert*-butyl-3-(3-(methoxycarbonyl)phenyl)-1*H*-indazole-1-carboxylate), based on compound **3**. No by-products were found with flash chromatography for all entries in this table.

2.10. Synthesis of 3-(1H-Indazole-3-yl)benzoic Acid (Compound **12***)*

As shown in Scheme 1, compound **12** was prepared by saponification and subsequent deprotection of compound **11,** according to the same process employed for the synthesis of compound **9** (Section 2.8). Compound **12** was obtained as a light yellow solid, the yield was 89%. Mp 244.8–245.4 °C. ^{1}H NMR (400 MHz, DMSO-d_6) δ_H, ppm: 13.37 (1H, s, COO*H*), 8.55 (1H, t, *J* = 1.8 Hz, Ar*H*), 8.21 (1H, dt, *J* = 1.5, 7.9 Hz, Ar*H*), 8.03 (1H, d, *J* = 8.2 Hz, Ar*H*), 7.95 (1H, dt, *J* = 1.4, 7.8 Hz, Ar*H*), 7.61 (2H, m, Ar*H*), 7.39 (1H, m, Ar*H*), 7.20 (1H, dd, *J* = 6.9, 8.0 Hz, Ar*H*) (Figure S24, Section S24, Supplementary Materials). ^{13}C NMR (101 MHz, DMSO-d_6) δ_C, ppm: 167.86, 142.77, 142.20, 134.62, 132.02, 131.36, 129.87, 128.93, 127.84, 126.81, 121.91, 120.84, 120.48, 111.35 (Figure S25, Section S25, Supplementary Materials). FT-IR (KBr) σ, cm^{-1}: 3627 (br m, N-H), 2926 (s, furyl ring), 1698 (m, C=O), 1618 (m, C=N), 1380 (w, C-N), 1235 (m, C-O). ESI-HRMS (TOF-SIMS, positive, *m*/*z*): 239.0807 (Calcd. for [M+H]$^+$ 239.2480) (Figure S26, Section S26, Supplementary Materials). Anal. Calcd. for $C_{14}H_{10}N_2O_2$: C, 70.58; H, 4.20; N, 11.76. Found: C, 70.97; H, 3.73; N, 12.03.

2.11. General Procedure for Catalytic Suzuki–Miyaura Coupling Reaction

2.11.1. Non-Ionic Liquid-Facilitated Reaction

As shown in annotations a-b of Tables 1–3, a mixture of compound **3** (1.0 mmol; Scheme 1; electrophile), compounds **4**, **7**, or **10** (1.2 mmol; Scheme 1; nucleophile), respectively, Pd catalyst (4 mol%, based on organic halide), anhydrous Na_2CO_3 (2.0 mmol), and THE solvent system (toluene, 4 mL; H_2O, 2 mL; EtOH, 1 mL) were combined into a round-bottom flask (100 mL) with a condenser and balloon, and then vigorously stirred at 80 °C for 8 h. When the time was up, the mixture was extracted with diethyl ether (3 × 50 mL), and the organic layers were combined and washed with saturated $NaHCO_3$ solution (50 mL),

distilled H_2O (50 mL), and brine (50 mL). After being dried over anhydrous Na_2SO_4 and filtration, the solution was concentrated under reduced pressure, and the residue was further purified using flash chromatography (SiO_2, 100–200 mesh; petroleum ether/ethyl acetate, 4/1, *v*/*v*; adding a few drops of triethylamine in eluent, 10 drops of triethylamine vs. 200 mL eluent), to give cross-coupling product (compound **5**, orange solid, R_f = 0.35; compound **8**, white solid, R_f = 0.62; compound **11**, light yellow solid, R_f = 0.50; all R_f values reported on TLC with the same eluent polarity as that used in flash chromatography).

2.11.2. Ionic Liquid-Facilitated Reaction

As shown in annotations a-b of Tables 1–3, compound **3** (1.0 mmol; Scheme 1; electrophile) and Pd catalyst (4 mol%, based on organic halide) were fully dispersed in imidazolium ILs ($BMImBF_4$ or $BMImPF_6$, 5 mL, respectively) in a round-bottom flask (100 mL) with a condenser and balloon under vigorous magnetic stirring at 25 °C. The mixture thus obtained was further stirred at 80 °C for 1 h, to achieve a uniform solution. Next, compounds **4**, **7**, or **10** (1.2 mmol; Scheme 1; nucleophile, respectively), anhydrous Na_2CO_3 (2.0 mmol), and THE solvent system (toluene, 4 mL; H_2O, 2 mL; EtOH, 1 mL) were added, and then the mixture was further stirred at 80 °C for 8 h. The resulting mixture was carefully concentrated under reduced pressure to remove all solvents, and the residue (IL-containing phase) was extracted using diethyl ether (3 × 50 mL). Organic layers (diethyl ether phases) were decanted and collected, washed with saturated $NaHCO_3$ solution (50 mL), distilled H_2O (50 mL) and brine (50 mL), dried over anhydrous Na_2SO_4, filtrated, and concentrated under reduced pressure. After TLC monitoring, flash chromatography (SiO_2, 100–200 mesh; petroleum ether/ethyl acetate, 4/1, *v*/*v*; adding a few drops of triethylamine, 10 drops of triethylamine vs. 200 mL eluent) afforded corresponding cross-coupled products (compounds **5**, **8**, **11**, Scheme 1). Alternatively, the remaining oil (IL-containing phase) in flask was reloaded with all consumed components (except for Pd catalyst and ionic liquid), and recycling was carried out under the same reaction conditions.

2.12. Computational Methods

All relevant geometries were fully optimized using B3LYP density functional theory (DFT) in conjunction with the self-consistent reaction field (SCRF) method. The Def2-SVP basis set was used in the optimization. After geometry optimization, harmonic vibrational analyses were performed at the same level, to confirm that each minimum had no imaginary frequency or that each transition state (TS) had only one imaginary frequency. The minimum energy path (MEP) was also traced using the intrinsic reaction coordinate (IRC) method, to ensure that each TS structure was correctly linked with two minima. The alkaline THE solvent system (toluene, 4 mL; H_2O, 2 mL; EtOH, 1 mL), Na_2CO_3 (2.0 mmol), ILs ($BMImPF_6$ or $BMImBF_4$, 5 mL) was used in the experiment. Accordingly, ethanol was selected as a compromise solvent in the computations. The implicit PCM solvent model was adopted to roughly evaluate the solvent effect on the reaction in ethanol (ε = 24.85). To refine energies, single-point energy computations were conducted at the PCM-B3LYP/Def2-TZVP level. Therefore, the total energy was the sum of the single-point energy and thermal corrections of 353.15 K. All computations were fulfilled with Gaussian 09 program [37]. All 3-D structures were generated with the CYLview program [38].

3. Results and Discussion

3.1. The C-3 Iodination and N-H Protection of 1H-indazole

According to previous studies, most functionalization of C-3 of 1*H*-indazole such as alkylation and arylation was carried out after the N-H group of 1*H*-indazole was protected or pre-substituted [34,39–42]. In this work, however, 1*H*-indazole was first iodized on the C-3 position without protecting the N-H group (Scheme 1) [34], but the subsequent Suzuki–Miyaura cross-coupling reaction required protection of the N-H group using $(Boc)_2O$ (Scheme 1). Additionally, as the reactivities of halogen substituents showed an order I >Br >>Cl (C–Cl = 96 kcal mol^{-1}; C–Br = 81 kcal mol^{-1}; C–I = 65 kcal mol^{-1}

for Ph-X unit) [43], iodization was selected over bromination and chlorination, in order to accelerate the cross-coupling reaction.

3.2. The Catalytic Suzuki–Miyaura Cross-Coupling Reaction

3.2.1. Effect of Substrate

Overall, most catalytic Suzuki–Miyaura cross-coupling reactions proceeded smoothly within 8 h, and poor to excellent outputs were obtained for the coupling of compound **3** (electrophile) with compounds **4**, **7**, and **10** (all nucleophiles, Tables 1–3). Herein, furyl of compound **4** represents a structure having excessive π-electrons [44], but, comparatively, the aryls of compounds **7** and **10** had deficient π-electrons [45]. Furthermore, the π-electron density on the aryl of compound **10** was lower than that of **7**, mainly due to **10** having an *m*-substituted methoxycarbonyl group, which was actually an *o*- and *p*-orienting substituent. Meanwhile, the nucleophilicity of aryl (heteroaryl) boronic acids (compounds **4**, **7**, **10**) came from the negative charge at the carbon of C-B bond [46]. However, there was no obvious and definite order of reactivity among compounds **4**, **7**, and **10** (Tables 1–3), and it seemed that the catalyst along with the solvent dominated the cross-coupling yields more than the substrate structure (Tables 1–3), which probably means the present catalytic system has a wide scope for substrates.

3.2.2. Effect of Catalyst

When compound **3** was coupled with compound **4** during fresh catalysis, the activities of various Pa catalysts showed the order $PdCl_2$(dtbpf) (averaged yield 86.66%, entries 13–15, Table 1) >$PdCl_2$(dppf) (averaged yield 86.33%, entries 10–12, Table 1) >$Pd(OAc)_2$ (averaged yield 42.33%, entries 4–6, Table 1) >$PdCl_2$ (averaged yield 38.00%, entries 7–9, Table 1) >$Pd(PPh_3)_4$ (averaged yield 16.33%, entries 1–3, Table 1). Furthermore, the catalytic cross-coupling of compounds **3** with **7** and **10** showed much the same order (Tables 2 and 3). Overall, the divalent Pd complexes ($PdCl_2$(dtbpf) and $PdCl_2$(dppf)) appeared better than the simple divalent Pd salts, such as $Pd(OAc)_2$ and $PdCl_2$, while the activity of the zero-valent Pd precursor ($Pd(PPh_3)_4$) was the lowest.

It was previously reported that the typical Suzuki–Miyaura catalytic cycle undergoes oxidative addition, transmetallation, and reductive elimination [21,47]. The catalytically active $Pd^{(0)}$ species are first generated in situ, coming from the $Pd^{(0)}$ or $Pd^{(II)}$ precursor (raw catalyst), and then oxidative addition of aryl halide ArX (electrophile) provides the Pd complex [ArPdXLn]. Next, the addition of [ArPdXLn] with the pre-added base (RO^- or OH^-) gives an [ArPdORLn] intermediate, which is quickly reacted with an organoboron compound Ar'$B(OH)_2$, leading to the diaryl complex [ArPdAr'Ln]. This procedure is summarized as transmetallation. Lastly, reductive elimination of the diaryl complex produces the biaryl product Ar–Ar', along with $Pd^{(0)}$ for recycling [21,47].

In association with the typical Suzuki–Miyaura cross-coupling mechanism, it can be seen that the $Pd(PPh_3)_4$, a zero-valent palladium precursor, could not afford sufficient catalytically-active $Pd^{(0)}$ species, probably because the PPh_3 ligands were not able to stabilize the [ArPdXLn] intermediate complex very well in the present work [47]. In comparison, employment of OAc^- and Cl^- as ligands of Pd raw catalysts yielded better outputs (respective entries 4–9 vs. 1–3, Tables 1–3). However, the ferrocene-based ligands derived from $PdCl_2$(dppf) and $PdCl_2$(dtbpf) had the best effect on the stabilizing [ArPdXLn] intermediate, finally leading to much improved catalytic efficiencies (respective entries 10–15 vs. 1–9, Tables 1–3).

3.2.3. Effect of Ionic Liquid

With the catalytic results obtained to that point, it was significant to test the effects of the ionic liquids, including on the catalytic outputs, as well as catalyst recovery and recycling. First of all, all Pd catalysts were highly soluble in both $BMImBF_4$ and $BMImPF_6$, and the resulting mixture could be fully dispersed into the THE solvent system under

vigorous magnetic stirring. These characters guaranteed the effects of "one-phase catalysis, two-phases separation" [48].

Next, for the cross-coupling of halogenated and protected indazole (compound **3**) with 2-furanboronic acid (compound **4**), the introduction of two imidazolium ILs increased the yields of coupled products in the reactions catalyzed by $Pd(PPh_3)_4$ (entries 2–3 vs. 1, Table 1), $Pd(OAc)_2$ (entries 5–6 vs. 4, Table 1), and $PdCl_2$ (entries 8–9 vs. 7, Table 1). The use of $BMImBF_4$ in association with $PdCl_2$(dppf) increased the yield of coupled product (entries 11 vs. 10, Table 1), but use of $BMImPF_6$ showed negative effects on the catalytic yields (entries 12 vs. 10, Table 1). On the other hand, employing either $BMImBF_4$ or $BMImPF_6$ along with $PdCl_2$(dtbpf) did not contribute to the catalytic outputs (entries 14–15 vs. 13, Table 1).

Therefore, it seemed that introduction of imidazolium ILs caused the coordination of N to Pd in the simple Pd salts ($Pd(PPh_3)_4$, $Pd(OAc)_2$, $PdCl_2$)-catalyzed reactions, probably leading to a more stable intermediate [ArPdXLn] (Pd complex) [47], further improving the catalytic yields. However, when the Pd catalysts contained sophisticated ligands, such as dppf and dtbpf, the original P-containing ferrocene-based ligands showed positive effects on stabilizing the catalytic intermediate, but the introduction of imidazolium ILs may affect this stability through coordination of N, sometimes decreasing the outputs.

When the substrate (nucleophile) was changed to 4-methoxycarbonylphenylboronic acid (compound **7**, Scheme 1) and 3-methoxycarbonylphenylboronic acid (compound **10**), use of two imidazolium ILs generally produced enhanced yields of cross-coupled products (Tables 2 and 3), which could be ascribed to the unique structural and coordinating properties of the ILs.

In the meantime, there was another reasonable explanation for the roles of $BMImBF_4$ and $BMImPF_6$ in the present catalysis. It was previously reported that the combination of 1-*n*-butyl-3-methylimidazolium bromide (BMImBr) with $Pd(OAc)_2$ in an alkaline environment produced 1-*n*-butyl-3-methylimidazol-2-ylidene (BMIy) complex of Pd (such as $PdBr_2(BMIy)_2$ and analogues), which showed a high activity in the Heck reaction [49]. This *N*-heterocyclic carbene (NHC) complex ($PdBr_2(BMIy)_2$) probably has influences on both the NHC and counterion (Br^-), facilitating various catalytic reactions [49]. Furthermore, no palladium metal particles ($Pd^{(0)}$ black) appeared in this work, probably indicating the formation of *N*-heterocyclic carbene (NHC) complex of Pd. On the basis of the above analysis, the possible formation of NHC complex of Pd in this work is proposed in Scheme 2.

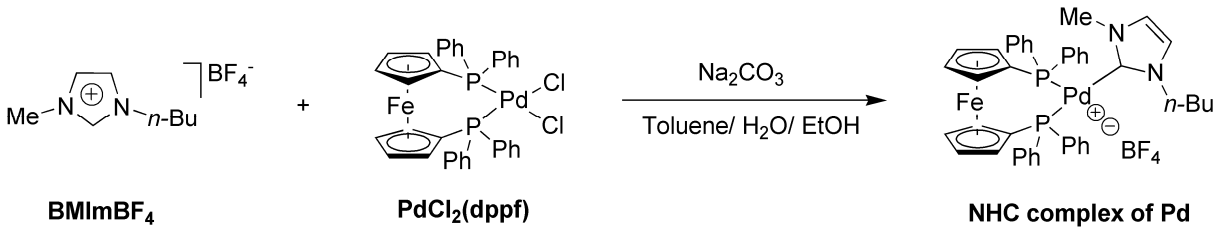

Scheme 2. Possible formation of NHC complex of Pd in this work.

3.2.4. Effect of Catalyst Recycling

The imidazolium ILs-facilitated catalyst recycling experiments are shown in Figures 2–4. In practice, several phenomena deserved attention. First of all, in the non-IL facilitated experiments, a lot of grey flakes appeared on the flask wall, which seemed to be amorphous $Pd^{(0)}$ black, but most of the IL-facilitated recycling reactions showed no $Pd^{(0)}$ black. Hence, the introduction of imidazolium ILs as recyclable media could stabilize the Pd intermediates, mainly due to coordination of N to Pd, which inhibited the formation of $Pd^{(0)}$ black and benefited the catalyst recovery (Figures 2–4) [50], or to the formation of the NHC complex of Pd (Scheme 2).

The performance of $BMImBF_4$ was usually much better than that of $BMImPF_6$ for the conversion of all substrates (respective a-d, Figures 2–4). Herein, BF_4^- was more hydrophilic than PF_6^- [29], which may show a better affinity to the base (Na_2CO_3) dissolved

in H_2O, probably stabilizing catalytic intermediates. Furthermore, taking into account the solubility of the solvent and its interaction with $BMImPF_6$ or $BMImBF_4$, some polar solvents such as diethyl ether, acetone, or DMF were able to extract cross-coupled products from ionic phases, but *n*-hexane was almost completely inert.

Moreover, the catalytic degradation of Pd-containing ionic liquids can be ascribed to the precipitation and coagulation of Pd complexes from $BMImPF_6$ or $BMImBF_4$. For instance, $PdCl_2$(dtbpf) combined with $BMImPF_6$ showed a 32% yield after being used four times (Figure 4d), where the ionic liquid layer became attenuated and the black solid coagulated and floated, probably leading to sharply declined outputs.

3.3. Theoretical Insights into the Catalytic Suzuki–Miyaura Cross-Coupling Mechanism

In order to further inspect the mechanism, the effective ligand dtbpf (entries 13–15, Table 3), compounds **3** and **10** (substrates **3** and **10**, Figure 5), were selected for computation using density functional theory (optimized structures are shown in Section S27, Supplementary Materials). As shown in Figure 5, the computational results indicated that, after the formation of the $Pd^{(0)}$ precatalyst, the reaction successively underwent oxidative addition, transmetalation, and reductive elimination. In particular, herein, there were three OH groups in the coordinated boronic acid (Int-3, Figure 5): two of them came from the coordinated boronic acid (compound **10**, Scheme 1), while the remaining one was derived from the alkaline reaction medium (Section 2.11), indicating that the P-Pd bond was hydrolyzed by OH^- in the alkaline reaction medium (Int-3, Figure 5), which propelled a further reaction (Figure 5). The final reductive elimination towards compound **11** (**substrate 11**, Figure 5) was the rate-determining step ($\Delta G^{\ddagger}$ = 10.1 kcal/mol). The overall reaction was strongly exothermic (ca. −70.5 kcal/mol). For comparison, an alternative ligand dppf (entries 10–12, Table 3) was also tested in the computations. It turned out that the barrier (17.3 kcal/mol) in the rate-determining step with dppf ligand was slightly higher than that with the dtbpf ligand.

As shown in Figure 6, the selected optimized structures showed that the bond angles of C-Pd-C in **Int-5** were 78° and 82° for dtbpf and dppf liands in the reductive elimination, demonstrating that it suffered more constraint from the steric repulsion of two *tert*-butyl groups than that of two phenyl groups. In this sense, more constraint from the ligand led to a shorter distance and lower barrier in the reductive elimination. Note that, on the contrary, the strong repulsion would increase the barrier of oxidative addition (1.7 vs. 6.5 kcal/mol, **TS1**, Figure 5), although this step was somewhat rapid and could not strongly disturb the overall mechanism.

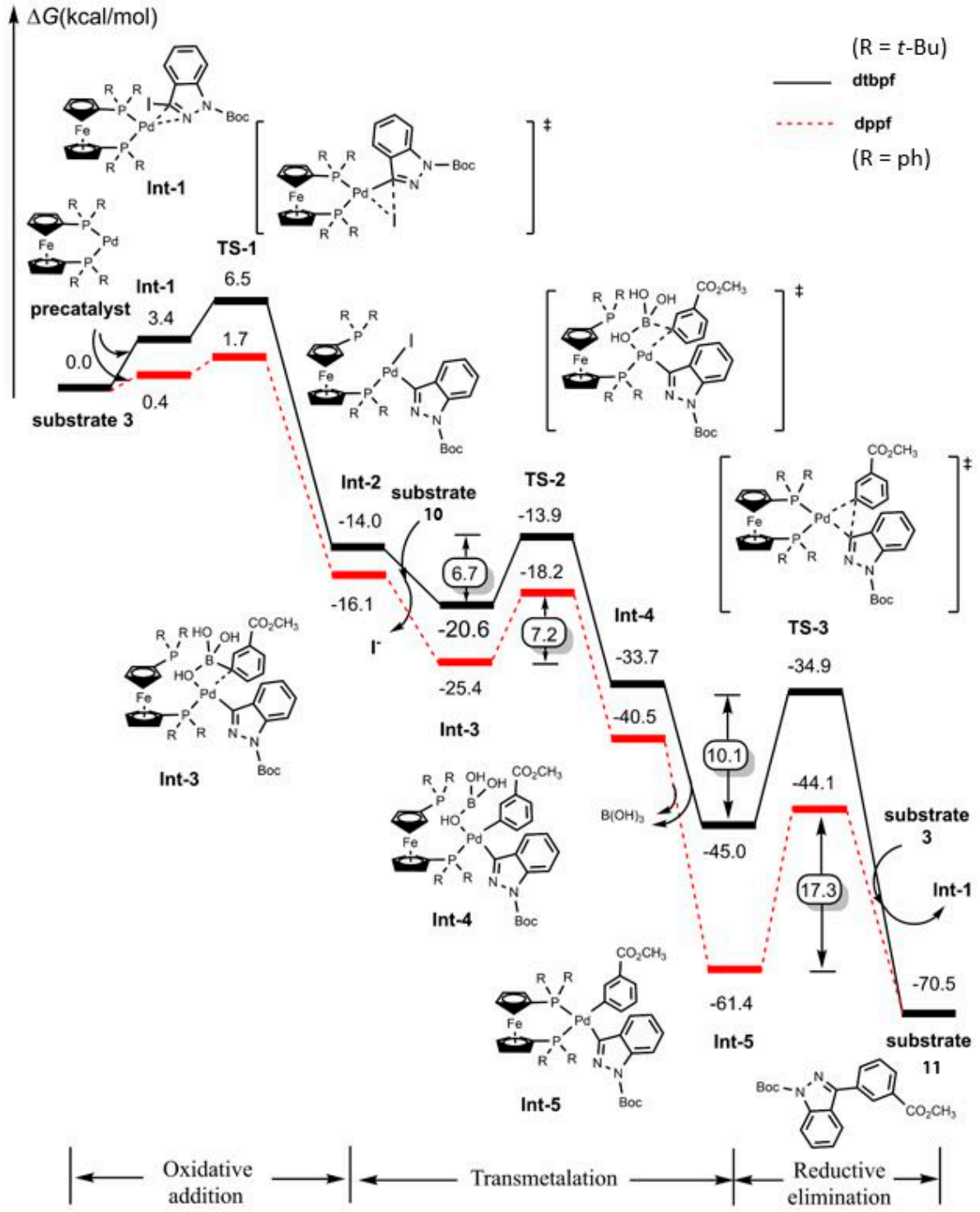

Figure 5. Relative Gibbs free energy (kcal/mol) profiles in Suzuki–Miyaura cross-coupling of compounds **3** with **10** to yield compound **11** using Pa catalyst featuring dtbpf (balck solid line) or dppf (red dashed line) ligands.

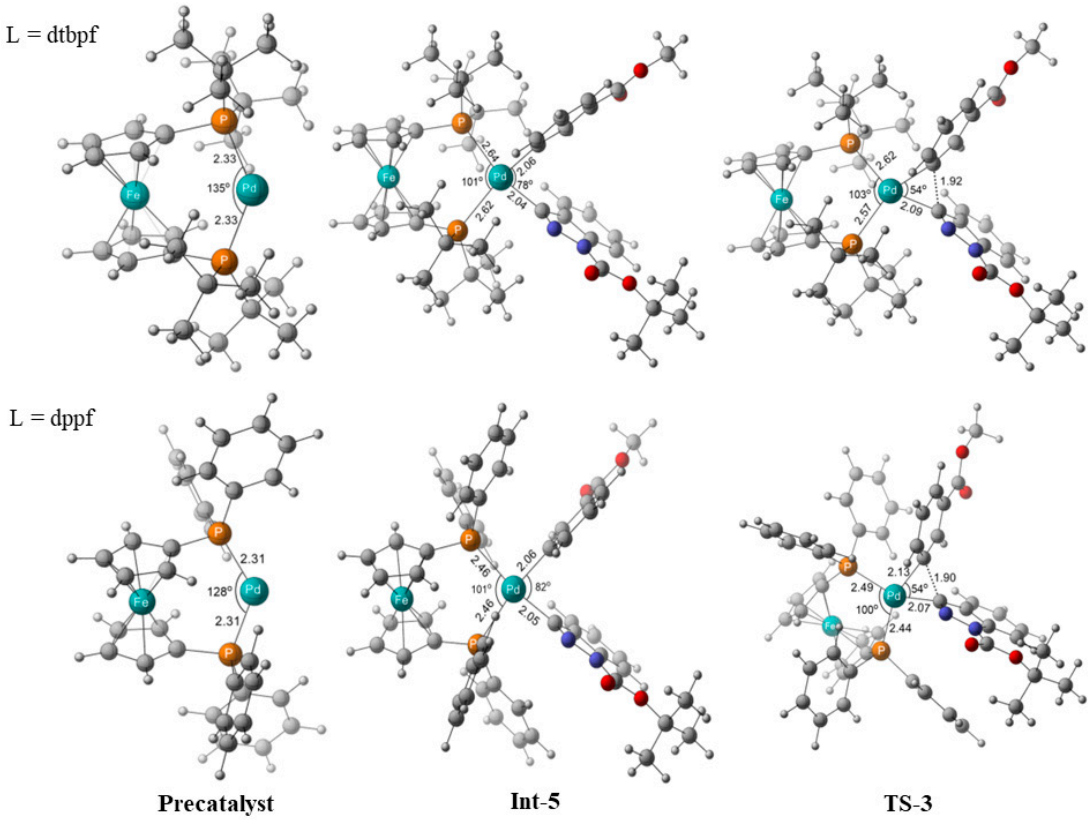

Figure 6. Selected optimized geometries of **Precatalyst**, **Int-5**, and **TS-3**. Bond distances in Å and angles in degrees.

4. Conclusions

In conclusion, this work presented the Suzuki–Miyaura cross-coupling reactions of a halogenated and N-H protected indazole (electrophile) with organic boronic acids (nucleophiles), catalyzed by different divalent palladium complexes, with or without imidazolium ionic liquids as functional or recyclable media, eventually leading to three C3-functionalized 1*H*-indazole derivatives. The series of reaction parameters were fully discussed. In general, the averaged catalytic activity of the Pd catalysts exhibited the order $PdCl_2$(dtbpf) >$PdCl_2$(dppf) >$Pd(OAc)_2$ >$PdCl_2$ >$Pd(PPh_3)_4$. Moreover, using two imidazolium ionic liquids generally improved the yields of cross-coupled products, as compared to those obtained from non-ionic liquid-facilitated reactions. The $BMImBF_4$ obviously performed better than $BMImPF_6$ for fresh catalysis and recycling, which could be related to the hydrophilicity of anions such as BF_4^- and PF_6^-. Meanwhile, use of $BMImBF_4$ and $BMImPF_6$ as recycling media could avoid the formation of $Pd^{(0)}$ black to a large extent, clearly enhancing the catalyst recovery and recycling. In addition, on the basis of scientific calculations, it was seen that the dppf ligand coming from $PdCl_2$(dtbpf) had four *tert*-butyl groups, which caused higher energy barriers during formation of the catalytic intermediates compared to those caused by dppf from $PdCl_2$(dppf), also illustrating a reason why $PdCl_2$(dppf) performed better than $PdCl_2$(dtbpf). This work put forward some new insights into the interactions of Pd catalysts with ionic liquids and showed the potential for the large-scale production of valuable 1*H*-indazole derivatives.

Supplementary Materials: The following supporting information can be downloaded at: https://www.mdpi.com/article/10.3390/app13074095/s1, Section S1: ^{1}H NMR spectrum of 3-iodo-1*H*-indazole (compound **2**) (Figure S1); Section S2: ^{13}C NMR spectrum of 3-iodo-1*H*-indazole (compound **2**) (Figure S2); Section S3: ^{1}H NMR spectrum of *tert*-butyl-3-iodo-1*H*-indazole-1-carboxylate (compound **3**) (Figure S3); Section S4: ^{13}C NMR spectrum of *tert*-butyl-3-iodo-1*H*-indazole-1-carboxylate (compound **3**) (Figure S4); Section S5: ESI-HRMS of *tert*-butyl-3-iodo-1*H*-indazole-1-carboxylate

(compound **3**) (Figure S5); Section S6: FT-IR spectrum of *tert*-butyl-3-iodo-1*H*-indazole-1-carboxylate (compound **3**) (Figure S6); Section S7: ^{1}H NMR spectrum of *tert*-butyl-3-(2-furyl)-1*H*-indazole-1-carboxylate (compound **5**) (Figure S7); Section S8: ^{13}C NMR spectrum of *tert*-butyl-3-(2-furyl)-1*H*-indazole-1-carboxylate (compound **5**) (Figure S8); Section S9: ESI-HRMS of *tert*-butyl-3-(2-furyl)-1*H*-indazole-1-carboxylate (compound **5**) (Figure S9); Section S10: FT-IR spectrum of ESI-HRMS of *tert*-butyl-3-(2-furyl)-1*H*-indazole-1-carboxylate (compound **5**) (Figure S10); Section S11: ^{1}H NMR spectrum of 3-(2-furyl)-1*H*-indazole (compound **6**) (Figure S11); Section S12: ^{13}C NMR spectrum of 3-(2-furyl)-1*H*-indazole (compound **6**) (Figure S12); Section S13: ^{1}H NMR spectrum of *tert*-butyl-3-(4-(methoxycarbonyl)phenyl)-1*H*-indazole-1-carboxylate (compound **8**) (Figure S13); Section S14: ^{13}C NMR spectrum of *tert*-butyl-3-(4-(methoxycarbonyl)phenyl)-1*H*-indazole-1-carboxylate (compound **8**) (Figure S14); Section S15: ESI-HRMS of *tert*-butyl-3-(4-(methoxycarbonyl)phenyl)-1*H*-indazole-1-carboxylate (compound **8**) (Figure S15); Section S16: FT-IR spectrum of *tert*-butyl-3-(4-(methoxycarbonyl)phenyl)-1*H*-indazole-1-carboxylate (compound **8**) (Figure S16); Section S17: ^{1}H NMR spectrum of 4-(1*H*-indazole-3-yl)benzoic acid (compound **9**) (Figure S17); Section S18: ^{13}C NMR spectrum of 4-(1*H*-indazole-3-yl)benzoic acid (compound **9**) (Figure S18); Section S19: ESI-HRMS (TOF-SIMS) of 4-(1*H*-indazole-3-yl)benzoic acid (compound **9**) (Figure S19); Section S20: ^{1}H NMR spectrum of *tert*-butyl-3-(3-(methoxycarbonyl)phenyl)-1*H*-indazole-1-carboxylate (compound **11**) (Figure S20); Section S21: ^{13}C NMR spectrum of *tert*-butyl-3-(3-(methoxycarbonyl)phenyl)-1*H*-indazole-1-carboxylate (compound **11**) (Figure S21); Section S22: ESI-HRMS of *tert*-butyl-3-(3-(methoxycarbonyl)phenyl)-1*H*-indazole-1-carboxylate (compound **11**) (Figure S22); Section S23: FT-IR spectrum of *tert*-butyl-3-(3-(methoxycarbonyl)phenyl)-1*H*-indazole-1-carboxylate (compound **11**) (Figure S23); Section S24: ^{1}H NMR spectrum of 3-(1*H*-indazole-3-yl)benzoic acid (compound **12**) (Figure S24); Section S25: ^{13}C NMR spectrum of 3-(1*H*-indazole-3-yl)benzoic acid (compound **12**) (Figure S25); Section S26: ESI-HRMS (TOF-SIMS) of 3-(1*H*-indazole-3-yl)benzoic acid (compound **12**) (Figure S26); Section S27: Optimized structures from calculations.

Author Contributions: Experimental and sample analysis, J.Y., A.Z. and L.J.; scientific calculation, Y.W.; material characterization, Q.P.; sample analysis and funding acquisition, X.W.; experiment design and methodology, X.L.; catalytic reaction, W.W.; experiment design and methodology, M.G.; conceptualization and original draft preparation, Y.S. All authors have read and agreed to the published version of the manuscript.

Funding: This work was supported by Natural Science Basic Research Program of Shaanxi Province (No. 2020JM-019).

Institutional Review Board Statement: Not applicable.

Informed Consent Statement: Not applicable.

Data Availability Statement: Not applicable.

Conflicts of Interest: The authors declare no conflict of interest.

References

1. Büchel, G.E.; Kossatz, S.; Sadique, A.; Rapta, P.; Zalibera, M.; Bucinsky, L.; Komorovsky, S.; Telser, J.; Eppinger, J.; Reiner, T.; et al. *cis*-Tetrachlorido-bis(indazole)osmium(IV) and its osmium(III) analogues: Paving the way towards the *cis*-isomer of the ruthenium anticancer drugs KP1019 and/or NKP1339. *Dalton Trans.* **2017**, *46*, 11925–11941. [CrossRef] [PubMed]
2. Yang, Z.; Yu, J.-T.; Pan, C. Recent advances in C–H functionalization of 2*H*-indazoles. *Org. Biomol. Chem.* **2022**, *20*, 7746–7764. [CrossRef] [PubMed]
3. Tandon, N.; Luxami, V.; Kant, D.; Tandon, R.; Paul, K. Current progress, challenges and future prospects of indazoles as protein kinase inhibitors for the treatment of cancer. *RSC Adv.* **2021**, *11*, 25228–25257. [CrossRef] [PubMed]
4. Yadav, L.; Chaudhary, S. Bu_4NI-catalyzed, oxidative $C_{(sp2)}$–$C_{(sp3)}$ cross dehydrogenative coupling for the regioselective direct C-3 benzylation of 2*H*-indazoles. *Org. Biomol. Chem.* **2020**, *18*, 5927–5936. [CrossRef] [PubMed]
5. Baraldi, P.G.; Balboni, G.; Pavani, M.G.; Spalluto, G.; Tabrizi, M.A.; De Clercq, E.; Balzarini, J.; Bando, T.; Sugiyama, H.; Romagnoli, R. Design, synthesis, DNA binding, and biological evaluation of water-soluble hybrid molecules containing two pyrazole analogues of the alkylating cyclopropylpyrroloindole (CPI) subunit of the antitumor agent CC-1065 and polypyrrole minor groove binders. *J. Med. Chem.* **2001**, *44*, 2536–2543. [CrossRef]
6. Qian, S.; Cao, J.; Yan, Y.; Sun, M.; Zhu, H.; Hu, Y.; He, Q.; Yang, B. SMT-A07 a 3-(indol-2-yl) indazole derivative, induces apoptosis of leukemia cells in vitro. *Mol. Cell. Biochem.* **2010**, *345*, 13–21. [CrossRef]

7. Ghosh, D.; Ghosh, S.; Ghosh, A.; Pyne, P.; Majumder, S.; Hajra, A. Visible light-induced functionalization of indazole and pyrazole: A recent update. *Chem. Commun.* **2022**, *58*, 4435–4455. [CrossRef]
8. Fustero, S.; Sánchez-Roselló, M.; Barrio, P.; Simón-Fuentes, A. From 2000 to mid-2010: A fruitful decade for the synthesis of pyrazoles. *Chem. Rev.* **2011**, *111*, 6984–7034. [CrossRef]
9. Ma, C.; Feng, Z.; Li, J.; Zhang, D.; Li, W.; Jiang, Y.; Yu, B. Photocatalytic transition-metal-free direct 3-alkylation of 2-aryl-2*H*-indazoles in dimethyl carbonate. *Org. Chem. Front.* **2021**, *8*, 3286–3291. [CrossRef]
10. Vidyacharan, S.; Ramanjaneyulu, B.T.; Jang, S.; Kim, D.-P. Continuous-flow visible light organophotocatalysis for direct arylation of 2*H*-indazoles: Fast access to drug molecules. *ChemSusChem* **2019**, *12*, 2581–2586. [CrossRef]
11. Sun, M.; Li, L.; Wang, L.; Huo, J.; Sun, M.; Li, P. Controllable chemoselectivity in the reaction of 2*H*-indazoles with alcohols under visible-light irradiation: Synthesis of C3-alkoxylated 2*H*-indazoles and *ortho*-alkoxycarbonylated azobenzenes. *Org. Chem. Front.* **2021**, *8*, 4230–4236. [CrossRef]
12. Park, B.Y.; Pirnot, M.T.; Buchwald, S.L. Visible light-mediated (hetero)aryl amination using Ni(II) salts and photoredox catalysis in flow: A synthesis of tetracaine. *J. Org. Chem.* **2020**, *85*, 3234–3244. [CrossRef] [PubMed]
13. Petrone, D.A.; Ye, J.; Lautens, M. Modern transition-metal-catalyzed carbon-halogen bond formation. *Chem. Rev.* **2016**, *116*, 8003–8104. [CrossRef]
14. Singsardar, M.; Dey, A.; Sarkar, R.; Hajra, A. Visible-light-induced organophotoredox-catalyzed phosphonylation of 2*H*-indazoles with diphenylphosphine oxide. *J. Org. Chem.* **2018**, *83*, 12694–12701. [CrossRef] [PubMed]
15. Geng, X.; Xu, Z.; Cai, Y.; Wang, L. Visible-light-driven multicomponent cyclization by trapping a 1,3-vinylimine ion intermediate: A direct approach to pyrimido[1,2-b]indazole derivatives. *Org. Lett.* **2021**, *23*, 8343–8347. [CrossRef] [PubMed]
16. Chan, E.Y.W.; Kir, S.; Tooze, S.A. siRNA screening of the kinome identifies ULK1 as a multidomain modulator of autophagy. *J. Biol. Chem.* **2007**, *282*, 25464–25474. [CrossRef] [PubMed]
17. Lazarus, M.B.; Novotny, C.J.; Shokat, K.M. Structure of the human autophagy initiating kinase ULK1 in complex with potent inhibitors. *ACS Chem. Biol.* **2015**, *10*, 257–261. [CrossRef]
18. Wood, S.D.; Grant, W.; Adrados, I.; Choi, J.Y.; Alburger, J.M.; Duckett, D.R.; Roush, W.R. In silico HTS and structure based optimization of indazole-derived ULK1 inhibitors. *ACS Med. Chem. Lett.* **2017**, *8*, 1258–1263. [CrossRef]
19. Clutterbuck, L.A.; Posada, C.G.; Visintin, C.; Riddal, D.R.; Lancaster, B.; Gane, P.J.; Garthwaite, J.; Selwood, D.L. Oxadiazolylindazole sodium channel modulators are neuroprotective toward hippocampal neurones. *J. Med. Chem.* **2009**, *52*, 2694–2707. [CrossRef]
20. Collot, V.; Varlet, D.; Rault, S. Heck cross-coupling reaction of 3-iodoindazoles with methyl acrylate: A mild and flexible strategy to design 2-azatryptamines. *Tetrahedron Lett.* **2000**, *41*, 4363–4366. [CrossRef]
21. Han, F.-S. Transition-metal-catalyzed Suzuki–Miyaura cross-coupling reactions: A remarkable advance from palladium to nickel catalysts. *Chem. Soc. Rev.* **2013**, *42*, 5270–5298. [CrossRef] [PubMed]
22. Beletskaya, I.P.; Alonso, F.; Tyurin, V. The Suzuki-Miyaura reaction after the Nobel prize. *Coord. Chem. Rev.* **2019**, *385*, 137–173. [CrossRef]
23. Miyaura, N. Cross-coupling reaction of organoboron compounds via base-assisted transmetalation to palladium(II) complexes. *J. Organomet. Chem.* **2002**, *653*, 54–57. [CrossRef]
24. Boit, T.B.; Weires, N.A.; Kim, J.; Garg, N.K. Nickel-catalyzed Suzuki–Miyaura coupling of aliphatic amides. *ACS Catal.* **2018**, *8*, 1003–1008. [CrossRef] [PubMed]
25. Wang, D.; Weinstein, A.B.; White, P.B.; Stahl, S.S. Ligand-promoted palladium-catalyzed aerobic oxidation reactions. *Chem. Rev.* **2018**, *118*, 2636–2679. [CrossRef]
26. Chernyshev, V.M.; Khazipov, O.V.; Eremin, D.B.; Denisova, E.A.; Ananikov, V.P. Formation and stabilization of nanosized Pd particles in catalytic systems: Ionic nitrogen compounds as catalytic promoters and stabilizers of nanoparticles. *Coord. Chem. Rev.* **2021**, *437*, 213860. [CrossRef]
27. Miyaura, N.; Suzuki, A. Palladium-catalyzed cross-coupling reactions of organoboron compounds. *Chem. Rev.* **1995**, *95*, 2457–2483. [CrossRef]
28. Zhang, Q.; Zhang, S.; Deng, Y. Recent advances in ionic liquid catalysis. *Green Chem.* **2011**, *13*, 2619–2637. [CrossRef]
29. Mathews, C.J.; Smith, P.J.; Welton, T. Palladium catalysed Suzuki cross-coupling reactions in ambient temperature ionic liquids. *Chem. Commun.* **2000**, 1249–1250. [CrossRef]
30. Lombardo, M.; Chiarucci, M.; Trombini, C. A recyclable triethylammonium ion-tagged diphenylphosphine palladium complex for the Suzuki–Miyaura reaction in ionic liquids. *Green Chem.* **2009**, *11*, 574–579. [CrossRef]
31. Mehnert, C.P.; Cook, R.A.; Dispenziere, N.C.; Afeworki, A.M. Supported ionic liquid catalysis-a new concept for homogeneous hydroformylation catalysis. *J. Am. Chem. Soc.* **2002**, *124*, 12932–12933. [CrossRef]
32. Muthayala, M.K.; Chhikara, B.S.; Parang, K.; Kumar, A. Ionic liquid-supported synthesis of sulfonamides and carboxamides. *ACS Comb. Sci.* **2012**, *14*, 60–65. [CrossRef]
33. Bocchi, V.; Palla, G. High yield selective bromination and iodination of indoles in *N*,*N*-dimethylformamide. *Synthesis* **1982**, 1096–1097. [CrossRef]
34. Collot, V.; Dallemagne, P.; Bovy, P.R.; Rault, S. Suzuki-type cross-coupling reaction of 3-iodoindazoles with aryl boronic acids: A general and flexible route to 3-arylindazoles. *Tetrahedron* **1999**, *50*, 6917–6922. [CrossRef]

35. Wentrup, C.; Benedikt, J. Nitrile imine and carbene rearrangements. From furfural to benzofulvene-8-carboxaldehyde, 8-benzofulvenylcarbene, and 1-vinylideneindene. *J. Org. Chem.* **1980**, *45*, 1407–1409. [CrossRef]
36. Vazquez, J.; De, S.K.; Chen, L.-H.; Riel-Mehan, M.; Emdadi, A.; Cellitti, J.; Stebbins, J.L.; Rega, M.F.; Pellecchia, M. Development of paramagnetic probes for molecular recognition studies in protein kinases. *J. Med. Chem.* **2008**, *51*, 3460–3465. [CrossRef] [PubMed]
37. Frisch, M.J.; Trucks, G.W.; Schlegel, H.B.; Scuseria, G.E.; Robb, M.A.; Cheeseman, J.R.; Scalmani, G.; Barone, V.; Mennucci, B.; Petersson, G.A.; et al. *Gaussian 09*; Revision, D.01; Gaussian, Inc.: Wallingford, CT, USA, 2009.
38. Legault, C.Y. CYLview, 1.0b; Université de Sherbrooke. 2009. Available online: http://www.cylview.org (accessed on 15 July 2022).
39. Ye, M.; Edmunds, A.J.F.; Morris, J.A.; Sale, D.; Zhang, Y.; Yu, J.-Q. A robust protocol for Pd(II)-catalyzed C-3 arylation of (1*H*) indazoles and pyrazoles: Total synthesis of nigellidine hydrobromide. *Chem. Sci.* **2013**, *4*, 2374–2379. [CrossRef] [PubMed]
40. Ben-Yahia, A.; Naas, M.; Kazzouli, S.E.; Essassi, E.M.; Guillaumet, G. Direct C-3-arylations of 1*H*-indazoles. *Eur. J. Org. Chem.* **2012**, *2012*, 7075–7081. [CrossRef]
41. Gambouz, K.; Abbouchi, A.E.; Nassiri, S.; Suzenet, F.; Bousmina, M.; Akssira, M.; Guillaumet, G.; Kazzouli, S.E. "On water" palladium catalyzed direct arylation of 1*H*-indazole and 1*H*-7-azaindazole. *Molecules* **2020**, *25*, 2820. [CrossRef]
42. Hattori, K.; Yamaguchi, K.; Yamaguchi, J.; Itami, K. Pd- and Cu-catalyzed C-H arylation of indazoles. *Tetrahedron* **2012**, *68*, 7605–7612. [CrossRef]
43. Grushin, V.V.; Alper, H. Transformations of chloroarenes, catalyzed by transition-metal complexes. *Chem. Rev.* **1994**, *94*, 1047–1062. [CrossRef]
44. Ackermann, M.; Pascariu, A.; Höcher, T.; Siehl, H.-U.; Berger, S. Electronic properties of furyl substituents at phosphorus and their influence on ^{31}P NMR chemical shifts. *J. Am. Chem. Soc.* **2006**, *128*, 8434–8440. [CrossRef]
45. Ribas, J.; Cubero, E.; Luque, F.J.; Orozco, M. Theoretical study of alkyl-π and aryl-π interactions. Reconciling theory and experiment. *J. Org. Chem.* **2002**, *67*, 7057–7065. [CrossRef]
46. Wang, J.; Zheng, W.; Ding, L.; Wang, Y. Computational study on C–B homolytic bond dissociation enthalpies of organoboron compounds. *New J. Chem.* **2017**, *41*, 1346–1362. [CrossRef]
47. Jana, R.; Pathak, T.P.; Sigman, M.S. Advances in transition metal (Pd,Ni,Fe)-catalyzed cross-coupling reactions using alkyl-organometallics as reaction partners. *Chem. Rev.* **2011**, *111*, 1417–1492. [CrossRef] [PubMed]
48. Yu, H.; Hu, J.; Fan, J.; Chang, J. One-pot conversion of sugars and lignin in ionic liquid and recycling of ionic liquid. *Ind. Eng. Chem. Res.* **2012**, *51*, 3452–3457. [CrossRef]
49. Xu, L.; Chen, W.; Xiao, J. Heck reaction in ionic liquids and the in situ identification of *N*-heterocyclic carbene complexes of palladium. *Organometallics* **2000**, *19*, 1123–1127. [CrossRef]
50. Slagt, V.F.; de Vires, A.H.M.; de Vires, J.G.; Kellogg, R.M. Practical aspects of carbon-carbon cross-coupling reactions using heteroarenes. *Org. Proc. Res. Dev.* **2010**, *14*, 30–47. [CrossRef]